Journal of Non-Oxide Glasses Vol. 7, No 3, 2015, p. 45 - 53

UV INDUCED OPTICAL AND STRUCTURAL INVESTIGATION OF THERMALLY EVAPORATED AMORPHOUS $Ge_6As_{38}Se_{56}$ THIN-FILM

R. CHAUHAN*
Department of Physic, DAV College, CSJM University, Kanpur (UP), India - 208001

Present study reports about structural and optical changes under UV exposure (i-line, g-line) on thermally evaporated amorphous $Ge_6As_{38}Se_{56}$ chalcogenide thin-film. Determination of linear optical absorption and linear refractive index is done using optical transmission spectra. Nonlinear refractive index is determined using semi-empirical relation. Changes in optical properties upon UV exposure are understood in terms of structural changes using Raman and XRD measurements. To understand the usability of investigated composition in the context of optical/photonic applications, the study is compiled with previous literature.

(Received July 23, 2015; Accepted September 25, 2015)

Keywords: Amorphous Chalcogenide; Optical properties; Thin-films; Semi-empirical relations; Raman Spectroscopy.

1. Introduction

Optical/photonic components fabricated using amorphous chalcogenide (a-chalcogenide) compositions typically require engineering of linear/nonlinear optical properties as desired by the context of an application. Due to photosensitive nature of a-chalcogenides, photo-treatment is among one of the highly applicable and widely used techniques to bring crucial transformations in the optical properties of these materials. Structural flexibility and high-lying lone pair p states in valance bonds are the basic reason behind photo-induced changes in amorphous chalcogenides. Systematic investigations of a given glassy system provide useful information for device fabrication with optimized features. Theory of network glasses plays important role in this regard. It derives various parameters of glassy system in terms of glass network connectivity. Here, the glass network connectivity is further given in terms of Mean Coordination number (MCN), where MCN is the sum of product of coordination number and atomic percentages of constituent elements.

Theories of network glasses are experimentally verified in Ge-As-Se glassy system due to its exceptionally large glass formation region, which allows the study of this system in a larger MCN range of compositions [1-6]. As reported in literature by many workers, it is possible to introduce up to 70 at.% of Arsenic and 50 at.% of Germanium into the glassy alloys to obtain amorphous nature of chalcogenide composition [7]. The theory of network glasses suggests three phases in Ge-As-Se glassy systems, which are flexible floppy phase, rigid and stressed-rigid phase. As reported by P. Boolchand, there exists a self-organized phase around rigid phase, where the compositions are rigid but stress free [4]. This phase is known as intermediate phase (IP). The compositions in this phase show non-ageing behavior, which is important from application point of view. In Ge-As-Se glasses, range of intermediate phase composition is $2.4 \leq \text{MCN} \leq 2.67$. However, the most useful compositions for applications such as all-optical-signal-processing lay in the range $2.4 \leq \text{MCN} \leq 2.5$ [8]. The selected thin-film sample is ternary a-$Ge_6As_{38}Se_{56}$ (MCN =

---

*Corresponding author: chauhanrasmi@gmail.com

2.5), which is at the upper limit of the MCN range of useful compositions mentioned above. The usability of these compositions is due to high linear/nonlinear refractive index, high third-order susceptibility, and thermal stability. In addition, presence of small number of wrong and defective bonds in these compositions results in low optical losses in IR region, which is a desirable property required in IR optical applications. In present work, optical and structural changes are investigated under low-intensity UV exposure for selected composition.

2. Experimental

In present study, bulk $Ge_{10}As_{40}Se_{50}$ (MCN = 2.6) glass is taken for investigation. It is expected that composition of thermally evaporated thin-film is different from bulk glass composition. In case of Ge-As-Se compositions, thermal evaporation causes over-stoichiometry of Se element and sub-stoichiometry of Ge and As elements. Fast deposition increases percentage of Se elements in thin-film. Hence, MCN of resulting thin-film becomes less than that of bulk glass. With $Ge_{10}As_{40}Se_{50}$ selected as bulk glass, useful thin-film compositions (MCN ≈ 2,5) can be expected at fast deposition rate.

To compose bulk $Ge_{10}As_{40}Se_{50}$ (MCN = 2.6) glasses using conventional melt quenching technique, the compositional elements Ge, As and Se with purity 99.99% were weighted according to their atomic percentages. These weighted elements were sealed in quartz ampoules at base pressure of 10^{-5} Torr. The quartz ampoules were heated inside a furnace up to 940°C at the rate of 3-4°C/min to prepare the melt. To obtain a homogeneous melt, the ampoules were frequently rocked for 10 hours at 940°C, and then quenched in ice water.

Thermal evaporation technique was used to prepare amorphous thin-films of glassy alloys onto cleaned glass substrates at room temperature inside a coating system (HIND-HIVAC Model 12A 4DT). The deposition rate was 10 to 15 nm/second. The films were exposed for different duration of time using Hg lamp through an optical arrangement, which filters out the light at two wavelengths (λ = 365 nm and λ = 436 nm, power density ~ 12.5 mW/cm^2). Amorphous natures of bulk samples and thin-films were verified using X-ray diffraction measurements (Thermo Electron Corporation, Model ARL X'TRA) with Cu Kα radiation, and a scan rate of 3°/minute. The compositional determination of thin-film was achieved using EDAX measurements (SUPRA 40VP Carl Zeiss NTS GmbH). The obtained chemical composition of thin-film was $Ge_{6.433}As_{37.688}Se_{55.880}$ (~ $Ge_6As_{38}Se_{56}$) [9].

Thicknesses of as prepared thin-films were measured experimentally using mechanical thickness profilometer (Tencore Instrument, Model Alpha Step 100). The optical transmissions for normal incidence of thin-films were measured using double beam UV/VIS computerized spectrophotometer (Hitachi, Model U-3310) in wavelength range of 300-900 nm.

For structural analysis, micro-Raman measurements were performed on a spectrometer (WITec, Alpha 300) using a 514.5 nm Argon ion laser with power density 5 mW/cm^2 at room temperature.

3. Results and discussion

3.1 XRD Analysis

XRD patterns of unexposed and 120 minutes UV exposed (i-line, g-line) thin-films are shown in Figure 1. Absence of any prominent peak in XRD patterns verifies amorphous nature of thin-films. The humps exhibited in XRD patterns verify small to medium range order in amorphous thin-films. Slight increase in sharpness of XRD pattern of exposed thin-film indicates that local structural changes are taking place. Local structural changes in the film under UV exposure are understood using Raman measurements in subsequent section.

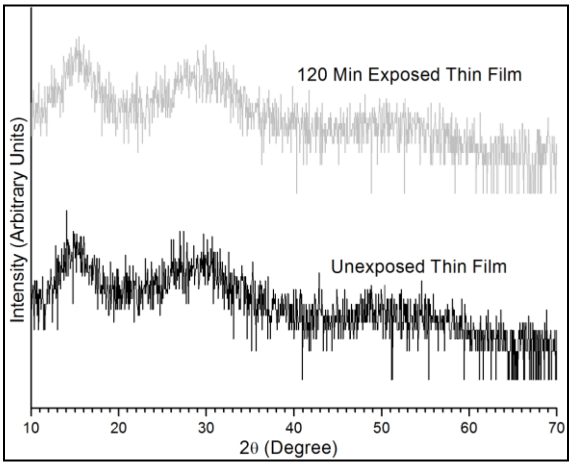

Fig. 1: XRD patterns of $Ge_6As_{38}Se_{56}$ *thin-films*

3.2 Optical Transmission Analysis

Determination of linear optical absorption coefficient is done from optical transmission (T) using Lambert-Beer's Law, which is given as T = exp(-αd), where, d is the thickness of the film (≈ 500 nm), and α is linear optical absorption constant. Variation of absorption coefficient with photon energy is shown in Figure 2. In low absorption region ($\alpha < 10^4$ cm^{-1}), it follows Urbach relation [10]. In high absorption region ($\alpha \geq 10^4$ cm^{-1}), it follows Tauc relation [11]. Thus, determination of optical bandgap is done using Tauc's plot for indirect bandgap material.

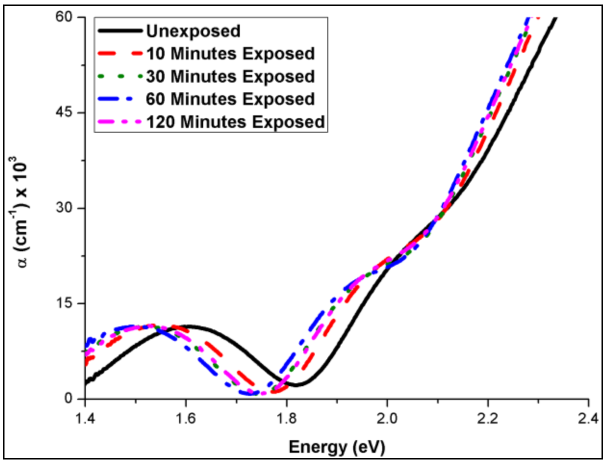

Fig. 2: Absorption Coefficients for $Ge_6As_{38}Se_{56}$ *thin-films*

From Table 1, little increase is observed in the value of optical bandgap for $Ge_6As_{38}Se_{56}$ thin-film at time scale of UV exposure. Previous studies report that changes in optical bandgap of a-Ge-As-Se compositions under photoexposure depend upon glass network structure, which is given in terms of MCN value. The MCN value changes with change in number of Ge and As atoms. Addition of Ge in glass network structure increases photobleaching, while addition of As enhance photodarkening [12-14]. It is also reported that compositions within MCN range of 2.4 to 2.55 have comparatively stable structural arrangement [5, 15]. Hence, studies of photoexposure on optical bandgap are reported by many research groups around this MCN range as described below.

G. Yang et al. reported that in ternary $Ge_xAs_{45-x}Se_{55}$ glassy system, Ge/As ratio plays important role in determination of photodarkening, photobleaching and photostability [16]. In this system, it is observed that photodarkening takes place at x = 0 ($As_{45}Se_{55}$, Ge/As = 0, MCN = 2.45), photo-bleaching takes place at x = 33 ($Ge_{33}As_{12}Se_{55}$, Ge/As = 2.75, MCN = 2.78), and photostability is achieved at x = 10 ($Ge_{10}As_{35}Se_{55}$, Ge/As = 0.286, MCN = 2.55). These investigations are performed under 660 nm insitu laser irradiation at power density 150 mW/cm^2. On the other hand, P. Nemec et al. reported that similar composition ($Ge_{10}As_{35}Se_{55}$) shows photo-bleaching under 660 nm laser irradiation at power density = 160 mW/cm^2, and composition $Ge_{20}As_{20}Se_{60}$ (MCN = 2.6, Ge/As = 1) is almost photostable under similar irradiation [17]. P. Nemec et al. explained this discrepancy on the basis of thin-film deposition process (PLD vs Thermal Evaporation) and deposition parameter (60 nm/min vs 3-4 nm/min) as fast deposition rate is responsible for change in stoichiometry and local structure of thin-film than bulk glass. In addition, P. Nemec reported that amorphous thin-films retains the stoichiometry, of bulk $Ge_{10}As_{40}Se_{50}$ glass, when films are deposited using PLD at slow deposition rate (3-4 nm/sec) and show photobleaching upon 660 nm laser exposure, as shown in Table 1.

Thin-film composition investigated by us is close to the $Ge_xAs_{45-x}Se_{55}$ glassy system of G. Yang et al. In addition, thin-film prepared in our experiment is prepared using thermal evaporation technique and deposition rate is fast. Hence, the behavior of thin-film sample seems to follow the theory of G. Yang et al based on Ge/As ratio approach.

Extinction coefficient (k) is a measure of light lost due to scattering and absorption per unit volume, and it is calculated using the relation:

$$k = \frac{\alpha\lambda}{4\pi} \tag{1}$$

It is observed in our studies that extinction coefficient decreases with wavelength as shown in Figure 3. Reduction of extinction coefficient with wavelength shows that material is getting transparent with wavelength. Hence, this composition is a useful optical material in high wavelength range.

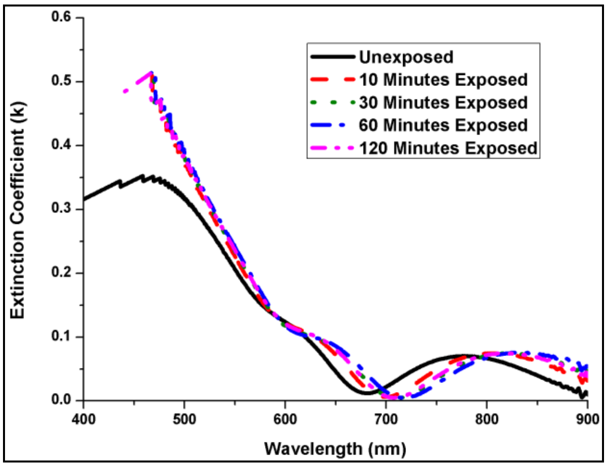

Fig. 3: Extinction Coefficients for $Ge_6As_{38}Se_{56}$ thin-films

Determination of linear refractive index (n_0) is done using the Dimitrov-Sakka relation [18, 19]:

$$[(n_0^2 - 1)/(n_0^2 + 2)] = 1 - (E_g/20)^{1/2} \tag{2}$$

It is clear from the Table 1 that negligible change occurs in the value of n_0 for $Ge_6As_{38}Se_{56}$ thin-films under UV exposure. It is also supported by XRD plots, which exhibit minimal structural changes. In a previous study reported by us for $As_{40}Se_{60}$ thin-films, it was observed that value of n_0 increases upon 30 minutes of i-line, g-line UV exposure, where intensity of incident radiation was similar to present study [14]. Hence, it can be concluded that addition of 6 at.% of Ge in binary As-Se alloy results in photostability of $Ge_6As_{38}Se_{56}$ thin-film.

Determination of nonlinear refractive index (n_2) can be done according to semi-empirical relation of Tichy et al., which is given as [20]:

$$n_2([esu]) \sim \frac{\overline{A}}{E_g^4} \tag{3}$$

where, $\bar{A} = 1.26\text{x}10^{-9}$ [esu $(eV)^4$]. Obtained values of n_2 as shown in Table 1 indicate that the value of nonlinear refractive index increases from $1.12\text{x}10^{-10}$ [esu] to $1.44\text{x}10^{-10}$ [esu] for 6 at.% Ge addition in As-Se alloy. UV exposure in a-$Ge_6As_{38}Se_{56}$ thin-films slightly reduces the value of n_2 from $1.44\text{x}10^{-10}$ [esu] to $1.37\text{x}10^{-10}$ [esu]. This is an indication of minor structural changes in the film.

Table 1: Linear/nonlinear refractive index and optical bandgap of a-Ge-As-Se thin-films with photo exposure

Composition	**Exposure**	**n**	**E_g (eV)**	**n_2 (Using Tichy Formula) (in 10^{-10} [esu])**
$As_{40}Se_{60}$ (MCN = 2.4)	Unexposed	2.31[14], 2.81 (hν→0)	1.79[14], 1.83[13]	1.22[14], 1.12
$As_{40}Se_{60}$ (MCN = 2.4)	30 min i-line, g-line exposed	2.48[14] (hν→0)	1.74[14]	1.37[14]
$As_{40}Se_{60}$ (MCN = 2.4)	120 min i-line, g-line exposed	2.85 (hν→0)	1.75[13]	1.34
$Ge_{10}As_{40}Se_{50}$ (MCN = 2.6)	Unexposed[17]	2.75 (at 1540 nm)	1.65	
$Ge_{10}As_{40}Se_{50}$ (MCN = 2.6)	660 nm laser[17]	2.69 (at 1540 nm)	1.75	
$Ge_{10}As_{30}Se_{60}$ (MCN = 2.5)	Unexposed[17]	2.64 (at 1540 nm)	1.77	
$Ge_{10}As_{30}Se_{60}$ (MCN = 2.5)	660 nm laser[17]	2.62 (at 1540 nm)	1.81	
$Ge_{15}As_{40}Se_{45}$ (MCN = 2.7)	Unexposed	2.75 (hν→0)	1.97[13]	0.84
$Ge_{15}As_{40}Se_{45}$ (MCN = 2.7)	120 min i-line, g-line exposed	2.73 (hν→0)	2.00[13]	0.79
$Ge_6As_{38}Se_{56}$ (MCN = 2.5)	Unexposed (Present Study)	2.87 (hν→0)	1.72[9]	1.44
$Ge_6As_{38}Se_{56}$ (MCN = 2.5)	10 min i-line, g-line exposed	2.86 (hν→0)	1.73[9]	1.41
$Ge_6As_{38}Se_{56}$ (MCN = 2.5)	30 min i-line, g-line exposed	2.86 (hν→0)	1.73[9]	1.41
$Ge_6As_{38}Se_{56}$ (MCN = 2.5)	60 min i-line, g-line exposed	2.86 (hν→0)	1.73[9]	1.41
$Ge_6As_{38}Se_{56}$ (MCN = 2.5)	120 min i-line, g-line exposed	2.86 (hν→0)	1.74[9]	1.38

3.3 Raman Analysis

Raman plots of unexposed and 120 minutes exposed a-$Ge_6As_{38}Se_{56}$ thin-films are shown in Figures 4 and 5. It can be observed in the figures that UV exposure slightly increases the sharpness of the curve. This is an indication of increase in local structural order, which occurs due to structural relaxation upon UV exposure. The change explains slight increase in optical bandgap upon exposure as shown in Table 1. Similar observations are noticed in XRD patterns shown in Figure 1, where the sharpness of the pattern slightly increases after the exposure.

The analysis of Raman measurement is done using the multi-peak fitting function of Origin 8.0. Raman plot of unexposed film exhibits three peaks centered at 192 cm^{-1} (Peak 1), 231 cm^{-1} (Peak 2) and 297 cm^{-1} (Peak 3). According to given literature, Peak 1 is assigned as A1 bond stretching mode of $GeSe_{4/2}$ corner sharing tetrahedral units, which is also known as υ_1 symmetric stretching vibration of $GeSe_{4/2}$ structural units [21-25]. Peak 2 is assigned as Main Band of As-Se glasses, which has the contribution of $AsSe_{3/2}$ pyramidal units, As-As bonds and As_4Se_3 cages [25-30]. Peak 3 is assigned as υ_3 asymmetric stretching vibration of $GeSe_{4/2}$ structural units [17, 21, 25]. It can be observed in Figure 4 and 5 that no new peaks are formed in the Raman spectra of the exposed film. It indicates that UV exposure (i-line, g-line) does not cause any chemical modification in amorphous chalcogenide thin-films. Only bonding rearrangements are taking place due to low-intensity UV exposure.

Shift in peak positions due to UV exposure (i-line, g-line) of 120 minutes is as follows. The first peak shifts from 192 cm^{-1} to 193 cm^{-1}, second peak from 231 cm^{-1} to 233 cm^{-1}, while position of third peak remains unchanged at 297 cm^{-1}. Relative areas and peak width of each of these peaks are shown in Table 2. From the table, it can be observed that relative area of peak 2 reduces from 0.793 to 0.758, while relative areas of Peak 1 and Peak 3 increase from 0.172 to 0.203 and 0.034 to 0.038. It indicates that UV exposure increases number of Ge-Se bonds and reduces number of As-Se and As-As bonds. According to chemical bond approach (CBA) theory, Ge-Se bonds are preferred over As-Se bonds because electronegativity difference between Se and Ge ($2.55 - 2.01 = 0.54$) is greater than that of Se and As ($2.55 - 2.18 = 0.37$). Hence, increase in Ge-Se bonds is an indication of structural relaxation upon UV exposure. In addition, the bond energy of Ge-Se bonds is greater than bond energy of As-Se and As-As bonds, hence, slight increase in Ge-Se bonds at the cost of As-Se and As-As bonds slightly increase the cohesive energy of the system. It results in slight increase in band gap as shown in Table 1. It is also observed that peak width of stoichiometric $GeSe_{4/2}$ units slightly decreases from 19.81 to 19.12. This small reduction is indication of small increase in order of the system.

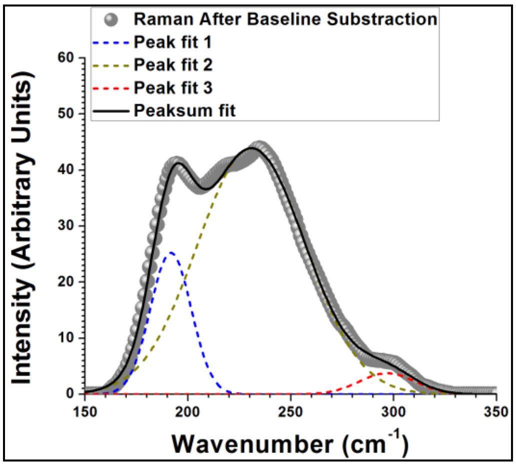

Fig. 4: Raman plot of unexposed thin-film

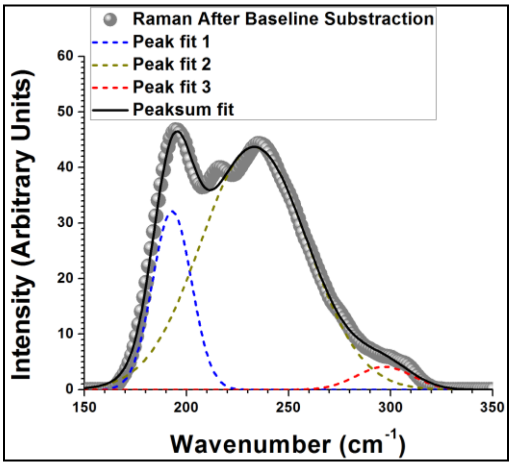

Figure 5: Raman plot of 120 minutes exposed thin-film

Table 2: Raman peak details of unexposed and 120 minutes exposed thin-films

Peak Details	Unexposed			120 minutes exposed		
	Peak Position (cm^{-1})	Width	Relative Area	Peak Position (cm^{-1})	Width	Relative Area
Peak 1: A1 bond stretching mode of $GeSe_{4/2}$ corner sharing tetrahedra	192	19.81	0.172	193	19.12	0.203
Peak 2: Main Band of As-Se glasses	231	52.63	0.793	233	52.32	0.758
Peak 3: υ_3 stretching vibration of $GeSe_{4/2}$ structural units	297	27.11	0.034	297	27.56	0.038

4. Conclusions

Findings of the present study about UV exposure (i-line, g-line, power density ~ 12.5 mW/cm^2) on intermediate phase a-$Ge_6As_{38}Se_{56}$ thin-film are given below:

1) Thin-film deposition using thermal evaporation of bulk a-$Ge_{10}As_{40}Se_{50}$ (MCN = 2.6) at fast deposition rate (10-15 nm/second) causes over-stoichiometry of Se element, whereas sub-stoichiometry of As and Ge elements. The resulting thin-film composition, as verified using EDAX is $Ge_6As_{38}Se_{56}$ (MCN = 2.5).

2) The thin-film shows slight increase in optical bandgap (1.72 to 1.74 eV) and almost negligible changes in linear refractive index (2.87 to 2.86) upon UV exposure. Small reduction in nonlinear refractive index ($1.44x10^{-10}$ to $1.38x10^{-10}$ [esu]) is also observed.

3) Raman analysis explains that UV exposure does not cause any chemical modification. It only causes bonding rearrangement i.e. increase in Ge-Se bonds and reduction in As-Se and As-As bonds, which is preferable bonding arrangement of this composition according to CBA theory. The cohesive energy of the film composition, as determined using CBA theory, increases when new bonding arrangement takes place due to UV exposure. The increase in cohesive energy is responsible for increase in optical bandgap.

4) Based on present study and available literature, it can be concluded that for binary As-Se compositions, photoexposure causes reduction in bandgap and increase in linear/nonlinear refractive index. While in case of ternary Ge-As-Se thin-films, nature of photoinduced changes depend on composition, Ge/As ratio, MCN value, thin-film preparation method and thin-film

deposition rate. Hence, all these parameters should be taken into account for optical engineering of ternary Ge-As-Se films using photoexposure.

Acknowledgement

Author wish to thank UGC, India for financial assistance via Project: F. No. 8-3 (99)/2011 (MRP/NRCB), Dr. Jitendra Kumar (Professor, MSP, IIT Kanpur, India) for optical measurements, Dr. P. K. Dwivedi (Sr. Scientific Officer, DST Unit on Nanosciences, IIT Kanpur, India) for Raman Measurements, and Dr. K. K. Srivastava (Associate Professor, DBS College, Kanpur, India) for fruitful discussions.

References

[1] J. C. Phillips, J. Non-Cryst. Solids, **34**(2), 153 (1979).
[2] M. F. Thorpe, D. J. Jacobs, B. R. Djordjevic, ed. P. Boolchand, World Scientific (2000).
[3] K. Tanaka, Phys. Rev. B, **39**(2), 1270 (1989).
[4] P. Boolchand, D. G. Georgiev, B. Goodman, J. Optoelectron. Adv. Mater. **3**, 703 (2001)
[5] D. A. P. Bulla, R. P. Wang, A. Prasad, A. V. Rode, S. J. Madden, B. Luther-Davies, Appl. Phys. A **96,** 615 (2009).
[6] R. P. Wang, C. J. Zha, A. V. Rode, S. J. Madden, B. Luther-Davies, J Mater Sci: Mater Electron, **18,** S419 (2007).
[7] Z. U. Borisova, Glassy Semiconductors, Plenum Press, Newyork (1981).
[8] A. Prasad, C.J. Zha, R. P. Wang, A. Smith, S. Madden and B. Luther-Davies, Opt. Express, **16**(4), 2804 (2008).
[9] A. Tripathi, R. Chauhan and K. K. Srivastava, International Conference on Recent Trends in Applied Physics and Material Science 2013, AIP Conference Proceedings, **1536**, 663 (2013).
[10] F. Urbach, Phys. Rev. **92**, 1324 (1953).
[11] J. Tauc, Amorphous and liquid semiconductors, New York: Plenum Press, (1979).
[12] Y. Kuzukawa, A. Ganjoo, K. Shimakawa, J. Non-Cryst. Solids, **227-23**0, 715 (1998).
[13] R. Chauhan, A. K. Srivastava, A. Tripathi, K. K. Srivastava, Prog. Nat. Sci.: Materials International, **20**(1), 54 (2010).
[14] R. Chauhan, A. K. Srivastava, A. Tripathi, and K. K. Srivastava, Prog. Nat. Sci.: Materials International, **21**(3), 205 (2011).
[15] B. Luther-Davies, Z. Congji, A. Prasad, and A. Smith, OSA Technical Digest Series (CD), paper CMGG7 (2007).
[16] G. Yang, H. Jain, A. Ganjoo, D. Zhao, Y. Xu, H. Zeng and G. Chen, Opt. Express, **16**(14), 10565 (2008).
[17] P. Nemec, S. Zhang, V. Nazabal, K. Fedus, G. Boudebs, A. Moreac, M. Cathelinaud, and X. H. Zhang, Opt. Express, **18**(22), 22944 (2010).
[18] V. Dimitrov, and S. Sakka, J. Appl. Phys. **79**(3), 1741 (1996).
[19] A. K. Srivastava and J. Kumar, AIP Advances, **1**(3), 032153 (2011).
[20] H. Tichá, L. Tichý, J. Optoelectron. Adv. Mater., **4**(2), 381 (2002).
[21] G. J. Ball, J. M. Chamberlain, J. Non-Cryst. Solids, **29**, 239 (1978).
[22] S. Sugai, Phys. Rev. B, **35**(3), 1345 (1987).
[23] A. Kumar, S. K. Tripathi, P. K. Kulriya, A. Tripathi, F. Singh, and D. K. Avasthi, J. Phys. D: Appl. Phys., **43**, 1 (2010).
[24] P. K. Dwivedi, S. K. Tripathi, A. Pradhan, V. N. Kulkarni, and S. C. Agarwal, J. Non-Cryst. Solids, **266-269**, 924 (2000).
[25] V. Q. Nguyen, J. S. Sanghera, J. A. Freitas, I. D. Aggarwal, and I. K. Lloyd, J. Non-Cryst. Sol., **248**, 103 (1999).
[26] P. K. Dwivedi, S. K. Sharma, A. Rammohan, and A. Sharma, 55th DAE Solid State Physics Symposium 2010, AIP Conference Proceedings, **1349**, 555 (2011).
[27] M. Frumar, Z. Polák, and Z. Černošek, J. Non-Cryst. Solids, **256-257**, 105 (1999).

[28] R. Ston, M. Vlcek, and H. Jain, J. Non-Cryst. Solids, **326-327**, 220 (2003).
[29] M. S. Iovu, E. I. Kamitsos, C. P. E. Varsamis, P. Boolchand, M. Popescu, Chalc. Lett. **2**(3), 21 (2005).
[30] K. Saitoh, O. Uemura, T. Usuki, and Y. Kameda, J. Non-Cryst. Solids, **192-193**, 286 (1995).